ARTICLES

Dynamics in the Early Stages of Decomposition in Liquid Nitromethane and Nitromethane−Diethylamine Mixtures

Ephraim Woods, III, Yury Dessiaterik, Roger E. Miller,* and Tomas Baer*

Department of Chemistry, University of North Carolina, Chapel Hill, North Carolina 27599-3290

Received: May 9, 2001; In Final Form: June 27, 2001

Laser-initiated decomposition of single aerosol particles in the source region of a time-of-flight spectrometer, followed by vacuum ultraviolet laser ionization and mass analysis of the reaction products, reveals the identity of species formed in the early stages of condensed-phase decomposition in nitromethane and nitromethane−diethylamine mixtures. In pure nitromethane, the initial stages of decomposition are characterized by unimolecular processes. At near-threshold energies, the cleavage of the C−N bond to form CH_3 and NO_2 dominates the dynamics, and at higher energies we find evidence of rearrangement to methylnitrite, followed by the formation of CH_3O and NO. In nitromethane seeded with 0.1% diethylamine, an additional channel is observed which produces ionic intermediates. Detection of protonated diethylamine and the nitromethane aci-anion confirm that an acid−base reaction is involved in this case. We also detect the radical anion, NO_2^-, whose production is correlated with an increase in methyl radical yield compared to the results for pure nitromethane. This correlation shows that NO_2^- is directly implicated in nitromethane decomposition. Furthermore, deuterium labeling studies indicate a hydrogen atom transfer reaction between the nitromethane aci-anion and neutral nitromethane that produces the weakly bound nitromethane anion, the precursor to CH_3 and NO_2^-. These data support and extend a sensitization mechanism proposed by Gruzdkov and Gupta [Gruzdkov, Y. A.; Gupta, Y. M. *J. Phys. Chem. A* **1998**, *102,* 2322] and discriminate against others.

Introduction

Understanding the mechanisms and dynamics of thermal and shock-induced decomposition is important in the development of new energetic materials such as rocket fuels. However, despite a great deal of research interest, little progress has been made in many of these systems because the problems are complex and the experiments are challenging. Many decomposition studies of energetic materials focus on gas-phase species since they are more accessible experimentally. These techniques include shock-initiated decomposition[1−3] and multiphoton dissociation.[4−6] While these studies are valuable in assessing the important unimolecular and isolated bimolecular decomposition pathways, they do not provide direct information about the condensed phase in which most of the important processes occur.

Mechanistic studies of condensed-phase decomposition are challenging for several reasons. Experimental techniques that rely on residual gas analysis typically do not have sufficient time resolution to monitor radical intermediates formed in the early stages of decomposition. Often, the identity of these important reaction intermediates can only be inferred. While techniques that employ optical spectroscopy in bulk material can monitor chemical changes with good time resolution, the inherently broad absorption bands make definitive identification of reaction intermediates problematic. In this paper, we describe a new technique for examining the mechanisms of condensed phase decomposition that uses a CO_2 laser to initiate the decomposition of aerosol particles in a vacuum. Because the particles have a large surface area-to-volume ratio and are located in a vacuum, reaction intermediates can escape the reaction zone and be detected readily with time-of-flight mass spectrometry (TOF-MS). Our first results in this effort concern the mechanism of amine sensitization of nitromethane.

Nitromethane (NM) is an important system to study because of its use as a fuel and the fact that it is a prototype molecule for a class of high-energy materials that includes trinitrotoluene (TNT). Also, its relative simplicity makes it an attractive subject for mechanistic studies. Gas-phase nitromethane has been studied using UV[7−9] and infrared[4,10] spectroscopy and shock tube studies.[1,2] Despite the fact that the literature on liquid state studies that include mechanistic information is quite extensive, there is little that is definitely known about the early stages of the liquid-state chemistry. Of particular interest is the interaction of nitromethane with amines. The addition of small amounts of amine to nitroalkyl compounds reduces the activation energy for detonation,[11] but the mechanism of this "sensitization" remains unknown 50 years after the discovery of the effect. The sensitization of nitromethane, in particular, has been the subject of much research, but there is very little agreement about the chemical mechanism. The goal of this work is to elucidate this mechanism through the direct observation of products from the earliest stages of the reaction.

In the first explanation for amine sensitization of nitromethane, Engelke et al.[12] suggested the importance of the aci-anion of nitromethane, $CH_2NO_2^-$, in the rate-limiting step of

* Corresponding authors. Fax: (919) 962-2388. E-mail: baer@unc.edu and remiller@unc.edu.

10.1021/jp0117765 CCC: $20.00
Published on Web 08/17/2001

detonation. Since the addition of amine, which acts as a base in nitromethane, increases the concentration of the aci-anion, it should result in sensitization. Their hypothesis is consistent with the observation that many different factors known to sensitize nitromethane, such as UV irradiation and high pressure, also produce the aci-anion.[13] However, they provided no direct evidence that the aci-anion is more reactive than neutral NM.[14] In a theoretical study, Politzer et al.[15] extended this hypothesis using density functional calculations and found that in the case of NH_3 sensitization, the most energetically favorable reaction pathway involves the aci-anion and the amine reaction:

$$[CH_2NO_2]^- + NH_3 \rightarrow CH_3NH_2 + NO_2^- \qquad (1)$$

The calculations showed that this reaction proceeds over a smaller activation barrier than the C−NO_2 bond cleavage in NM and produces a net release of energy. An important element of this reaction is that it produces another amine that can sustain the reaction.

Other studies question the importance of the aci-anion in the sensitization mechanism. Constantinou et al.[14] used differential scanning calorimetry to evaluate empirical sensitization factors that compare thermal decomposition rates of sensitized NM to that of pure NM for several NM/amine mixtures. Because these empirical factors do not correlate well with the basicity of the amines (and thus the aci-anion concentration), the authors suggested that the aci-anions do not play a role in the sensitization mechanism. Instead, they proposed that a charge-transfer complex between NM and the amine is responsible for weakening the C−N bond. On the basis of ab initio calculations, Cook and Haskins[16] suggested that a hydrogen-bonded complex, rather than a charge-transfer complex, is responsible for decreasing the C−N bond energy and promoting alternate reaction pathways. However, Politzer et al.[15] reported that these hydrogen bonded complexes do not appreciably change the C−N bond energy, concluding that they are unlikely to be important to the chemistry.

Revisiting the aci-anion hypothesis, Blais et al.[17] monitored the gaseous reaction products of a detonated liquid mixture of NM and 5% diethylenetriamine using time-of-flight mass spectrometry (12 ms resolution). Their sample dimensions (5 mm × 12 mm) exceeded the failure diameter of this compound so that the reaction produced the real detonation products, including some higher molecular weight adducts. However, fragmentation of the ions in the electron impact ionization source prevented a clear identification of these high-mass products. In addition, they found no evidence for the $CH_2NO_2^-$ ion.

In a different experiment, Gupta and co-workers measured time-resolved visible absorption spectra of shocked, liquid NM[18] and NM−amine mixtures[19] with a time resolution of 60 ns. This time resolution was sufficient to detect transient intermediates in the early stages of nitromethane decomposition. They found a transient signal unique to amine-sensitized mixtures whose peak absorption wavelength is approximate 500 nm and attributed this absorption to the radical anion, $CH_3NO_2^-$. They argued that this radical anion is formed from the NM aci-anion according to the reaction scheme:

$$CH_3NO_2 + RNH_2 \rightarrow CH_2NO_2^- + RNH_3^+ \qquad (2)$$

$$CH_2NO_2^- + CH_3NO_2 \rightarrow CH_3NO_2^- + CH_2NO_2 \qquad (3)$$

The first step in this process is the acid/base reaction which produces the NM aci-anion, $CH_2NO_2^-$. The aci-anion then reacts with a neighboring NM molecule forming the NM anion, $CH_3NO_2^-$. This species has a much weaker C−N bond than does NM (66 kJ/mol in the gas phase, as compared to 260 kJ/mol); therefore, it dissociates much more easily:

$$CH_3NO_2^- \rightarrow CH_3 + NO_2^- \qquad (4)$$

The rate-limited step of this process is reaction 2, and a kinetic analysis finds its activation energy to be 70 kJ/mol. While the wavelength of the intermediate's absorption band and the kinetics of its formation are consistent with their scheme, such broad absorption features cannot be unambiguously assigned.

In view of the sparse evidence for any of the chemical species involved in the early stages of NM detonation, no consensus exists for the mechanism for amine sensitization of nitromethane. The ability to observe reaction intermediates with high sensitivity makes aerosol mass spectroscopy uniquely capable of detecting the new chemical species introduced by the addition of amines to nitromethane. In this paper, we present mass spectra that identify the primary reaction products of unsensitized nitromethane (NM), as well as nitromethane sensitized with diethylamine (DEA). We also investigate NM−aniline mixtures as an added experimental control because aniline is an amine which is known to be a weak base and a poor sensitizer. There are clear differences in these results that point to differences in the chemical mechanisms. We then examine the product yields of these reactions as a measure of the relative reaction rates in order to verify that the new chemical species we observe in the sensitized mixtures is related to the sensitization mechanism. Last, we show experimental results from using isotopically labeled (deuterated) samples in order to monitor a critical hydrogen atom transfer step during the course of reaction. Taken together, these data provide clear and compelling support for the mechanism proposed by Gruzdkov and Gupta.[19]

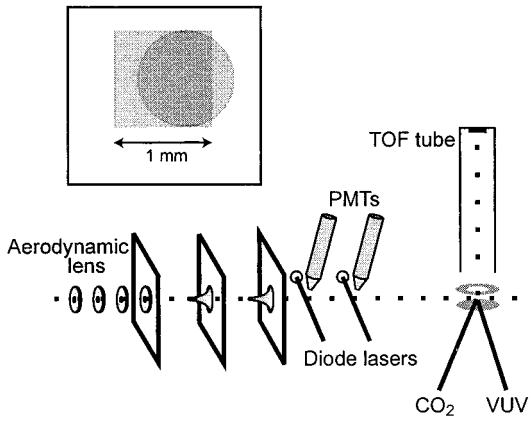

Figure 1. Schematic diagram of the experimental apparatus. It consists of an aerodynamic lens inlet, two stages of differential pumping, a light-scattering station for particle sizing and laser timing, and a time-of-flight mass spectrometer. The inset shows the overlap of the CO_2 (square) and VUV (circle) laser beams.

Experimental Section

The arrangement of this experiment is similar to that described in previous papers from this laboratory[20,21] and is inspired by the aerosol time-of-flight mass spectrometers used by several groups for on-line analysis of atmospheric aerosol particles.[22−24] Figure 1 shows a schematic diagram of the apparatus. The system comprises an aerodynamic lens inlet, two stages of differential pumping, a light scattering station, and a laser-based time-of-flight mass spectrometer. An aerosol particle (∼1−3 mm diameter) from an external stream enters the aerodynamic lens through a 100 μm, flow-limiting orifice. The aerodynamic

lens inlet, based on the design of McMurray[25,26] and Worsnop,[27] consists of a series of orifices of successively decreasing diameter. The lens focuses aerosol particles onto a well-defined axis, greatly increasing the efficiency with which they are detected. The focused particles accelerate through two stages of differential pumping to speeds between 60 and 200 m/s before entering the main a vacuum chamber. The particles then pass through two 532 nm diode laser beams placed 10 cm apart. Separate photomultiplier tubes detect the scattered light from each diode laser, and a digital timing circuit calculates the velocity of the particle based on the time delay between the two scattered light signals. The circuit then triggers the pulsed lasers to fire when the particle arrives in the spectrometer.

A pulsed TEA-CO_2 laser (Lumonics), which produces 0.2−0.8 J/pulse of light near 10.6 μm, concurrently initiates the chemistry in the aerosol particle and vaporizes it. After a delay of approximately 1 ms, a 118.5 nm vacuum ultraviolet (VUV) laser beam, produced by frequency-tripling 20 mJ of the 355 nm output of a Nd:YAG laser (Continuum) in a Xe gas cell, ionizes the vapor cloud for time-of-flight mass analysis. The VUV laser can ionize all neutral species with ionization energies (IE) less than 10.5 eV, the laser photon energy. It is interesting to note that ions that are present in the aerosol particle are directly promoted to the gas phase when the IR laser vaporizes the aerosol particle and therefore do not require the VUV laser for detection. It is possible to distinguish ionic species in the aerosol from neutral ones by comparing spectra obtained using both lasers with those obtained from only the CO_2 laser. This is an important consideration because the chemistry we observe in the amine sensitized mixtures produces both neutral and ionic reaction products. However, the detection efficiencies for pre-existing ions and neutral species ionized by the VUV laser are very different. Neutral species can be detected quantitatively over a range of concentrations,[28] while the detection efficiency for the pre-existing ions depends strongly on the ion concentration in the aerosol particle. This nonquantitative aspect of ion detection is a result of ion recombination during the vaporization step.[29]

A digital oscilloscope (HP, Infinium) digitizes each mass spectrum and transfers them to a PC through a GPIB connection. While the experiment operates at an average frequency of 10 Hz, aerosol particles arrive in the chamber at irregular intervals. If the digital timing circuit receives no light scattering signals within 100 ms, it fires the CO_2 laser and the flashlamps of the Nd:YAG laser to maintain their temperatures. These blank firings produce empty spectra since the lasers do not hit a particle. The data collection software sorts out the empty time-of-flight spectra after the data collection is complete. Typically, we record a single mass spectrum by transferring 500 single-particle spectra to the PC and averaging the 100−250 spectra that contain data. Since the ionization energy of the starting material, NM, is greater than the photon energy of our VUV laser, the VUV laser only produces ions when a chemical reaction has occurred. This is an important advantage since it eliminates the possibility of confusing fragment ions arising from the ionization of NM to real reaction products.

The absorption of radiation by the particle and the subsequent partitioning of that energy into molecular translational and internal energy is a complex problem, and a detailed description of these dynamics is beyond the scope of this article. However, a simple linear absorption model assuming an infrared cross section of 1×10^{-19} cm^2 predicts that radiation on the order of 10^{-9}−10^{-10} J is absorbed by the particle. Since the particle's mass is on the order of 4×10^{-12} grams, the laser provides sufficient energy to raise the particle's temperature by several hundred to several thousand Kelvins over the range of laser fluences accessible in our experiment. This result is consistent with the kinetic energy measurements we have made under similar vaporization conditions in nonreactive systems.[20] Future work will determine the internal energy of molecules in the vapor plume by analyzing the photoionization fragmentation patterns of trace, nonreactive molecules.

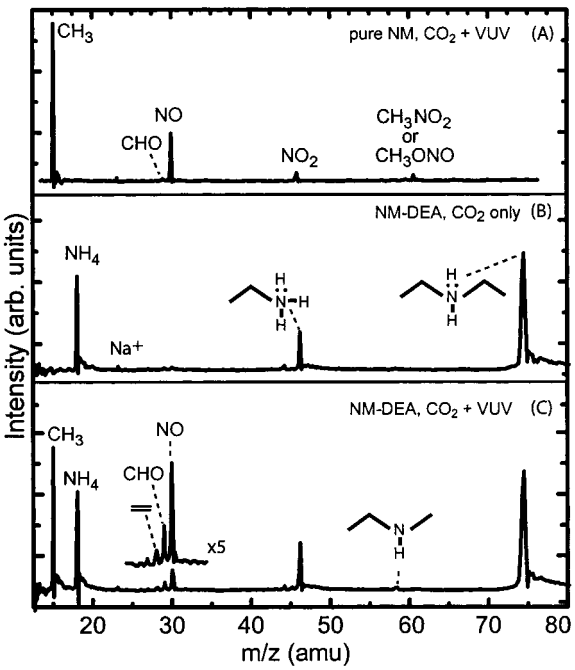

Figure 2. Positive ion mass spectra for (a) pure NM recorded with both the CO_2 and VUV lasers, (b) NM−DEA recorded with only the CO_2 laser, and (c) NM−DEA recorded using both the CO_2 and VUV lasers.

Results and Discussion

1. Identification of Reaction Products—Pure Nitromethane. Figure 2a shows a positive ion mass spectrum recorded by rapidly heating unsensitized (pure) NM particles with the CO_2 laser and using the VUV laser to ionize the neutral products of the reaction that evolve into the gas phase. The predominant feature in the mass spectrum corresponds to CH_3, while the smaller features correspond to NO, NO_2, and CH_3NO_2 (or CH_3-ONO). On the basis of these assignments, we conclude that the unsensitized NM decomposition initiates by the following two reactions:

$$CH_3NO_2 + \text{heat } (CO_2 \text{ laser}) \rightarrow CH_3 + NO_2 \quad (5)$$

$$\rightarrow CH_3ONO \rightarrow CH_3O + NO \quad (6)$$

Reaction 5, the homolytic cleavage of the C−N bond, has been found to be the initial step in the gas-phase decomposition,[1,2] and there is inconclusive evidence that the same is true for the liquid-phase decomposition.[18] Our measurements support this conclusion. The signals associated with the CH_3 radical (IE = 9.84 eV) are stronger than those for NO_2 (IE = 9.6 eV) because of the more favorable Franck−Condon factors for ionization in the former. In fact, the vertical excitation ionization threshold for NO_2 is 11.2 eV,[30] which is well above the laser photon energy of 10.5 eV. This channel (reaction 5) is the major component of our signal at all CO_2 laser fluences above the reaction threshold.

The appearance of NO in the spectrum is evidence for reaction 6, in which the rearrangement of nitromethane to methyl nitrite is followed by dissociation to CH_3O (IE = 10.7 eV) and NO (IE = 9.24 eV). Although we do not find clear evidence of the CH_3O product because its IE is higher than the energy of the VUV radiation, the small feature at $m/z = 29$ may be attributable to ionization of vibrationally excited CH_3O followed by rapid decay to CHO^+. We also observe a small peak at $m/z = 61$, which may result from either the rearrangement product CH_3ONO (IE = 10.4 eV) or highly vibrationally excited CH_3NO_2 (IE = 11.2 eV) molecules. This rearrangement reaction is well-known in the gas phase for nitromethane,[4] as well as other nitro compounds such as TNT,[31] and is much more facile than direct cleave of the N−O bond in NM. We detect the NO radical only at CO_2 laser fluences at least 30−50% larger than the threshold for detecting the $CH_3 + NO_2$ channel, consistent with its production by a higher activation energy process than simple C−N cleavage. This fact is consistent with the gas-phase results of Zhang and Bauer;[32] however, Wodtke et al. find that the nitrite isomerization channel competes with C−N bond rupture in IR multiphoton dissociation.[10] Since this channel is not implicated in the amine-sensitization mechanism and because it proceeds over a higher energy barrier than the C−N cleavage channel, it is not the primary focus of the present work. There are other likely reaction products, for example, CH_4, C_2H_6, and HONO, that, if present, would not appear in this mass spectrum because their ionization energies are higher than the energy of the VUV photons. The small signal from Na^+ arises from a small amount of $NaNO_3$ impurity obtained from the glass nebulizer used to create the NM aerosol. The Na^+ ions are an example of the pre-existing ions in the particle, and they are directly promoted into the gas phase by the CO_2 laser. This "ion evaporation" process is unimportant in the case of pure NM results; we will show that it is crucial in the analysis of the NM−amine mixtures because the mechanism is ionic in nature.

2. Identification of Reaction Products—NM−DEA Mixture. The results for pure nitromethane provide a good reference point for examining the NM−DEA system. Since we expect that the reaction of nitromethane sensitized with amine proceeds via a different chemical mechanism than does the reaction of pure NM, we anticipate that new chemical species will be formed that are unique to the NM−amine system. As a result, our first goal is to identify reaction products that are unique to the NM−amine system. As we discussed in the Experimental Section (and observed for the Na^+ impurity), pre-existing ions can be promoted directly into the gas phase by the CO_2 laser, and we can detect these ions without using the VUV laser. The same is true for ionic reaction products formed early in the decomposition. Therefore, comparing the positive ion mass spectrum obtained by firing just the CO_2 laser to that obtained by firing both the CO_2 and VUV lasers allows us to distinguish between the ionic and neutral products of the reaction. Panels b (CO_2 laser alone) and c (both CO_2 and VUV lasers) of Figure 2 show the results of this analysis for a NM−DEA mixture (0.1% DEA by volume).

As shown in Figure 2b, the major positively charged ionic products of the reaction are the three protonated amines, $(C_2H_5)_2NH_2^+$ (DEA-H^+), $C_2H_5NH_3^+$, and NH_4^+. The observation of the protonated amine at m/z 74, is a direct confirmation of reaction 2. Replacing NM with deuterated NM in this experiment produces DEA−d^+ ($m/z = 75$), confirming that the extra proton comes from the nitromethane molecule, as suggested in reaction 2. The protonated ethylamine and ammonium ion in Figure 2b are clearly the decomposition products of DEA−H^+ according to the following mechanism:

$$(C_2H_5)_2NH_2^+ \rightarrow C_2H_5NH_3^+ + C_2H_4 \rightarrow NH_4^+ + 2C_2H_4 \quad (7)$$

This ethene elimination channel for protonated amines is well-known in the gas phase.[33] We verified this reaction sequence by studying the intensity of these features as a function of CO_2 laser power. The intensity pattern for these three peaks shift from 100% $(C_2H_5)_2NH_2^+$ at low CO_2 laser energy to nearly 100% NH_4^+ at higher energies. The direct observation of the protonated amine and its decomposition products not only verifies the presence of these species in heated NM−DEA, it also demonstrates that they are the only positively charged ionic products in this reaction, an important consideration in formulating the chemical mechanism.

The bottom trace in Figure 2 shows, in addition to the ionic species, the neutral products of the reaction, CH_3, NO, C_2H_4, and CHO (or C_2H_5). There is also a small feature at $m/z = 58$ that arises from the VUV ionization of neutral, unreacted DEA. As pointed out before, it is not possible to measure the absolute concentration of the pre-existing ions (or their concentration relative to the neutral species) on the basis of the intensity of the ion signals. It is quite possible that the concentration of CH_3 radicals is much larger than that of the ionic species, which at most compose only 0.1% of the mixture. At this stage, our goal is to simply identify the reaction products. Aside from C_2H_4, which is a product of the DEA−H^+ decomposition, and the unreacted neutral DEA, these are the same neutral reaction products observed for the unsensitized nitromethane. Therefore, the only new chemical species that we detect are ionic, and these new species can be markers of an alternative chemical mechanism. However, the only ionic species in the positive ion spectrum are the protonated amine and its decomposition products. These species are involved in a simple unimolecular decay process (reaction 7) and are unlikely to play a major role in the sensitization mechanism. The existence of DEA−H^+, coupled with the observation that the extra proton is donated by NM, implies the existence of the NM aci-anion, $CH_2NO_2^-$, which has been implicated in the sensitization mechanism by several groups.[12,15,19,34]

Since the reaction of the nitromethane−amine mixture produces positive ions, it must also produce negative ions. Changing the polarity of the extraction plates in the spectrometer permits the collection of the negative ion mass spectrum, analogous to the positive ion spectrum shown in Figure 2b. The VUV laser only produces positive ions and electrons, so it is not used at all in the negative ion experiments. Figure 3 shows the negative ion mass spectrum for three separate samples: pure NM (a), NM + 0.1% aniline (b), and NM + 0.1% DEA (c). We have investigated aniline and diethylamine in order to observe the effect of basicity. In aqueous solution, aniline is slightly acidic with a pK_b of 9.1,[35] while diethylamine has a pK_b of 3.16.[35] The three major features in this spectrum are $m/z = 62$, 46, and 42. These peaks remain unchanged upon replacing nitromethane with NM-d_3 and, therefore, do not contain hydrogen atoms from the nitromethane. Therefore, we assign the features as NO_3^-, NO_2^-, and CNO^- respectively. As shown in inset of Figure 3c, we observe the NM aci-anion, $CH_2NO_2^-$, at a larger DEA concentration of 5%. This feature is weak compared to DEA−H^+ in the positive ion spectrum, perhaps because it is reactive at the energies of this experiment. Since the pure nitromethane spectrum contains Na^+ ions as an impurity, we expect that there are counterion impurities in the negative ion spectrum. As shown in the mass spectrum in Figure

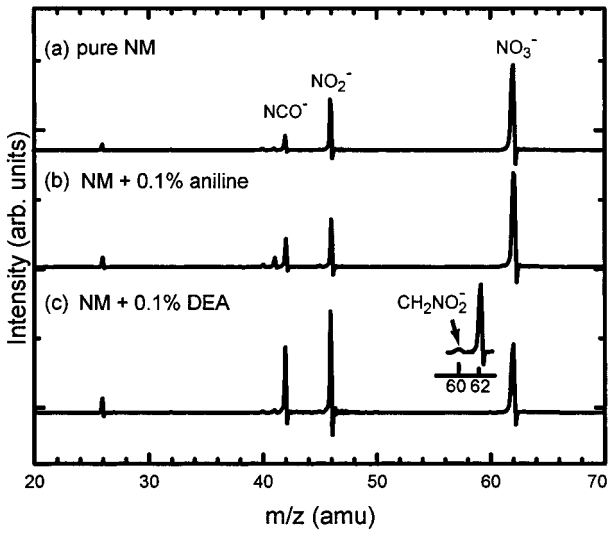

Figure 3. Negative ion mass spectra for (a) pure NM, (b) NM−aniline (0.1%), and (c) NM−DEA (0.1%). The inset in panel c shows the portion of the mass spectrum for NM−DEA (5%) that contains the $CH_2NO_2^-$ species ($m/z = 60$).

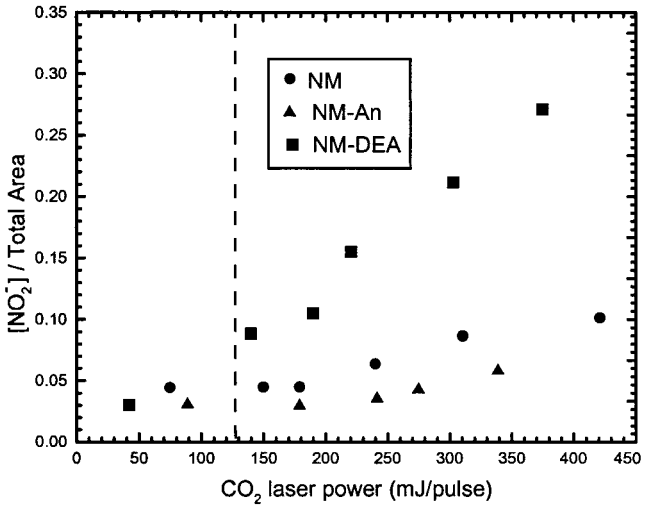

Figure 4. Integrated intensity of NO_2^- (normalized to total integrated intensity) vs CO_2 laser power for three different samples: NM (●), NM−aniline (▲), and NM−DEA (■). The vertical line indicates the lowest CO_2 laser power for which we observe methyl radicals in the corresponding positive ion mass spectrum.

3a, the major negative ions we observe, especially NO_3^-, are consistent with nitrate contaminants from our glass nebulizer. It is unfortunate that the NO_2^- species is among these since it is also an expected product from both the Gupta (reaction 4) and Politzer (reaction 1) mechanisms. However, the larger intensity of the NO_2^- feature for the NM−DEA mixture compared to the other two suggests that NO_2^- is a product of a reaction unique to that mixture. A negative ion mass-spectrum of pure DEA shows a strong CNO^- feature accounting for the larger CNO^- signal in the NM−DEA mixture, but the pure DEA spectrum shows no NO_2^- peak. The latter must therefore be a result of the interaction of NM with DEA.

By recording the mass spectra for pure NM, NM + 0.1% aniline, and NM + 0.1% DEA as a function of the CO_2 laser power, we find that the NO_2^- signal has a power dependence in the NM−DEA mixture different than that in the CNO^- and NO_3^- signals. Figure 4 charts the ratio of the NO_2^- signal to the total integrated signal for each sample as a function of the CO_2 laser power. It is evident that the relative intensity of the NO_2^- feature increases with laser power in the NM−DEA mixture, providing further evidence that it is a reaction product from NM and DEA. At low CO_2 laser power, there is insufficient energy to drive a chemical reaction, only enough to evaporate the aerosol particle. Thus, ionic impurities appear in the spectrum even for low laser fluences. The high temperatures required to initiate a chemical reaction, on the other hand, are reached only at the higher laser fluences. The vertical line in Figure 4 marks the lowest CO_2 laser power for which we observe methyl radicals in the positive ion spectrum for NM/DEA mixture. The onset of the production of the NO_2^- ion with increasing CO_2 laser power thus coincides with the reaction threshold energy. Since the onset of this growth is consistent with the threshold energy for the reaction, we conclude that the NO_2^- is a reaction product and that it is correlated with the methyl radical formation.

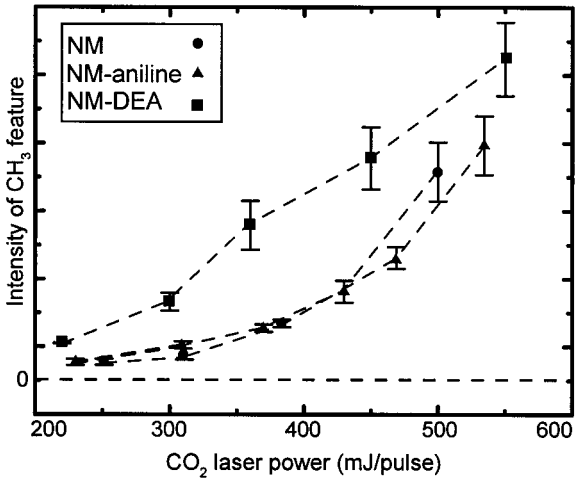

Figure 5. Integrated intensity of methyl radicals vs CO_2 laser power for three different samples: NM (●), NM−aniline (▲), and NM−DEA (■).

3. Methyl Radical Yields. Several groups have suggested that the creation of the $CH_2NO_2^-$ species, and therefore the basicity of the amine, is an important factor in determining the degree of sensitization.[15,19,34] In accord with that suggestion, we observe that the NM−DEA system produces reaction products (e.g., NO_2^-) different than either NM or the NM−aniline mixture. To confirm that these observations are related directly to the role of DEA in the sensitization mechanism, we compare the production of the CH_3 radical for each of the mixtures as a function of CO_2 laser power. Because the combustion reaction is ultimately sustained by free radicals, the CH_3 radical signal serves as a good indicator or "thermometer" for the extent of reaction. Figure 5 shows the integrated CH_3 ion intensity as a function of CO_2 laser power for the three different samples, NM, NM−aniline, and NM−DEA. To avoid the effects of differences in laser alignment and detection efficiency, we recorded all of the spectra used in this analysis consecutively, in a single day. Clearly, as the power of the CO_2 laser increases and more energy is available to drive the reaction, the intensity of the CH_3 radical feature grows for each sample. This increase in CH_3 concentration shows that the rate of CH_3 production increases with CO_2 laser power. While we cannot identify a CO_2 laser power for which the nitromethane−DEA mixture produces CH_3 radicals and pure nitromethane does not (mostly owing to large shot-to-shot fluctuations in CO_2 laser intensity), the plot shows that the yield of CH_3 radicals from the nitromethane−DEA mixture is higher than that for either of the other two samples at a given energy. We also note that the power dependence of the NM−DEA sample has a distinctly different shape than those of the other two samples. The methyl

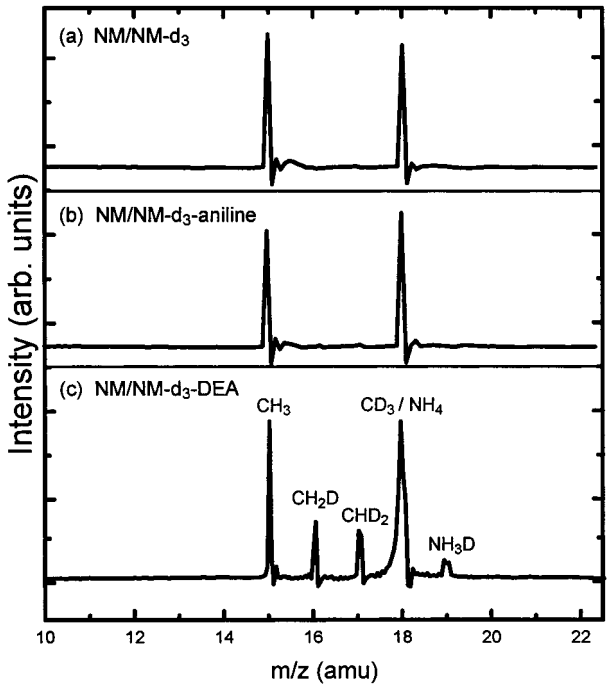

Figure 6. Expanded portion of positive ion mass spectrum for (a) NM + NM-d_3 (50%), (b) NM + NM-d_3 (50%) + aniline (0.1%), and (c) NM + NM-d_3 (50%) + DEA (0.1%).

radical intensity from NM−DEA grows nearly linearly with laser power, whereas the other two have higher-order dependence. This interesting behavior may be the subject of future studies.

From these data, we find that the rate of the reaction that produces the methyl radical is higher for the NM−DEA mixture than for the other two samples at a given laser delay and CO_2 laser energy. We conclude that a different chemical mechanism must be responsible for the increased rate of the reaction. The observation of unique reaction products for NM−DEA, especially NO_2^-, coupled with the greater rate of methyl radical production, strongly suggests that the chemistry that produces the NO_2^- is related to the sensitization mechanism. We can further conclude that since NM−aniline neither produces new reaction products nor increases the rate of methyl radical formation, aniline is a poor sensitizing agent, as has previous been shown for a molecule of similar basicity, *N*-methylaniline.[19]

4. Deuterium Substitution. The observation of the protonated DEA and the production of the NO_2^- species provide strong support of the Gupta mechanism. On the other hand, we find no evidence for $CH_3NO_2^-$ and only observe the aci-anion, $CH_2NO_2^-$, at large amine concentrations (~5%). The difficulty in observing $CH_2NO_2^-$ and $CH_3NO_2^-$ ions could be a result of their high reactivity and, thus, low concentration. To test the Gupta mechanism more directly, we turn to deuterium labeling studies. The critical step (reaction 3) involves the hydrogen/deuterium transfer between $CH_2NO_2^-$ and CH_3NO_2, the extent of which we can monitor mass spectrometrically. Figure 6 shows an expanded portion of the positive ion mass spectrum for three samples: NM, NM−DEA (0.1%), and NM−aniline (0.1%). In these samples, however, 50% of the nitromethane is deutereated (NM-d_3). We use these samples to illustrate the exchange of H atoms during the course of the reaction.

Figure 6a shows the result from NM/NM-d_3 in the absence of the amine. The only two features observed in this case are CH_3 and CD_3. The intensities are similar, which is consistent with a small deuterium effect for this simple homolytic bond breaking step. The C−N bond strength for nitromethane is nearly identical to that of NM-d_3, and one would not expect noticeably different reactivities for the two. Figure 6b shows the corresponding results for the NM−aniline sample. This spectrum is similar to the NM/NM-d_3 spectrum, indicating that aniline does not promote alternative reaction pathways that involve hydrogen atom exchange. This finding is consistent with the previous results demonstrating aniline's inability to sensitize this reaction. Last, Figure 6c displays the results from the NM/NM-d_3−DEA sample. In this case, there are additional mass peaks corresponding to CH_2D and CHD_2. (We note that the feature at $m/z = 18$ is a combination of CD_3 and NH_4^+, which comes from the decomposition of DEA−H^+ described earlier. This "ion evaporation" component to the signal causes it to be broad and asymmetric because the NH_4^+ ion is accelerated in the weak electric field prior to the application of the extraction pulse.

The intensity pattern for the methyl radical features in the NM/NM-d_3−DEA sample is about 3:1:1:3 (CH_3:CH_2D:CHD_2:CD_3). This pattern is constant throughout the course of the experiment, which we begin immediately after preparing the mixture. The observed products do not come entirely from the DEA-sensitized reaction. The production of methyl radicals arises from both the direct C−N bond rupture, as in pure NM, and from the sensitized reaction path that involves the amine. As shown in Figure 5, the increase in methyl radical signal in the amine-sensitized mixtures, compared to pure NM, depends on the CO_2 laser power. The data in Figure 6 were obtained with a CO_2 laser power (300 mJ/pulse) for which the NM−DEA mixture produces about twice the concentration of methyl radicals that pure NM produces, implying that the sensitized reaction accounts for approximately 50% of the methyl radical yield. The unsensitized reaction has an isotope pattern given by: 1:0:0:1 (see mass spectra in Figure 6a,b). By subtracting this weighted pattern from the NM/NM-d_3−DEA data in Figure 6, we conclude that the isotopic pattern for the sensitized reaction is approximately 1:1:1:1.

Isotopic scrambling could occur in two reactions. If the acid−base reaction between NM and DEA (reaction 2) were such as to reach equilibrium, the distribution should be 1:3:3:1, assuming that the only source of hydrogen and deuterium are the NM and NM-d_3, the DEA concentration being only 0.1%. We thus conclude that this equilibrium is not established. Another reaction scheme that could be responsible for isotopic mixing in the methyl radical species is reactions 3 and 4. The corresponding combinations of reaction steps for the deuterated species are

$$CH_2NO_2^- + CH_3NO_2 \rightarrow CH_3NO_2^- + CH_2NO_2 \rightarrow \mathbf{CH_3} + NO_2^- \quad (8)$$

$$CH_2NO_2^- + CD_3NO_2 \rightarrow CH_2DNO_2^- + CD_2NO_2 \rightarrow \mathbf{CH_2D} + NO_2^- \quad (9)$$

$$CD_2NO_2^- + CH_3NO_2 \rightarrow CD_2HNO_2^- + CH_2NO_2 \rightarrow \mathbf{CD_2H} + NO_2^- \quad (10)$$

$$CD_2NO_2^- + CD_3NO_2 \rightarrow CD_3NO_2^- + CD_2NO_2 \rightarrow \mathbf{CD_3} + NO_2^- \quad (11)$$

It is evident that in the absence of any kinetic isotope effects, a 50:50 mixture of CH_3NO_2 and CD_3NO_2, should produce a

1:1:1:1 isotope distribution in the methyl radicals. Our observed distribution of 1:1:1:1 thus provides direct evidence for the reactions 3 and 4 in the Gupta mechanism.

5. Reaction Thermochemistry. Sensitization of the NM reaction is achieved by producing radicals that can sustain a chain reaction via a lower activation energy mechanism than the homolytic C−N bond cleavage in CH_3NO_2. The comparison of the energetics is not simple because a number of critical pieces of data are not known. The reaction enthalpies for the relevant gas-phase species, as derived from standard heats of formation and electron/proton affinities, are the following:

$$CH_3NO_2 \rightarrow CH_3 + NO_2 \qquad \Delta H_{rxn,gas} = 260 \text{ kJ/mol}^{36} \quad (12)$$

$$CH_3NO_2 + DEA \rightarrow CH_2NO_2^- + DEA{-}H^+ \qquad \Delta H_{rxn,gas} = 523 \text{ kJ/mol}^{36-38} \quad (13)$$

$$CH_2NO_2^- + CH_3NO_2 \rightarrow CH_3NO_2^- + CH_2NO_2 \qquad \Delta H_{rxn,gas} = 237 \text{ kJ/mol}^{36,37,39,40} \quad (14)$$

$$CH_3NO_2^- \rightarrow CH_3 + NO_2^- \qquad \Delta H_{rxn,gas} = 66 \text{ kJ/mol}^{36,37,41} \quad (15)$$

It would appear from the above that the sensitization of the NM combustion by the acid base reaction 13 with its 523 kJ/mol endothermicity is highly improbable. However, in the condensed phase, solvation energies can greatly reduce the reaction enthalpy. For example, in aqueous solution, where the $pK_a(NM) = 10.2$ and the $pK_b(DEA) = 2.98$, the equilibrium constant for reaction 13 is approximately 7. The thermodynamics of this acid−base equilibrium in nitromethane solution are unknown, but we can guess that the enthalpy for reaction 13 lies somewhere between the gas phase and the aqueous phase values. The absence of complete statistical scrambling of the H/D atoms in our experiment indicates that the reaction does not equilibrate at room temperature prior to our analysis, so that the enthalpy must very positive. As pointed out by Blais et al.,[17] the reaction volume becomes an important factor in condensed phase reactions. From this point of view, the aci-ion formation (reaction 13) is favored over the simple dissociation reaction (reaction 12). It is not clear from our results whether the small $DEA{-}H^+$ and $CH_3NO_2^-$ concentrations present at room temperature are responsible for the chemistry we observe. It is possible that the energy from the CO_2 laser excitation drives the equilibrium toward the right-hand side of reaction 13, increasing the concentration of the critical aci-anion.

Likewise, it is difficult to determine what effect the solvent may have on the H atom transfer reaction (reaction 14). Gruzdkov and Gupta suggest that this is the rate-limiting step in their mechanism, and estimate its activation energy as 70 kJ/mol. As shown above, the gas phase value for this reaction is much higher, essentially the difference in electron affinities of CH_3NO_2 and CH_2NO_2. This disparity must arise from the solvation energy of the ionic products.

Conclusion

We directly observe reaction products from the initial stages of decomposition in NM and NM−amine mixtures, and these products clearly indicate the reaction mechanisms in each case. For pure NM, the initial stages of the decomposition appear to be dominated by unimolecular processes. The predominant pathway at the energies of our experiment is the direct cleavage of the C−N bond, producing the CH_3 radical and NO_2. We also find evidence for a higher-energy channel involving rearrangement of the NM parent to methyl nitrite followed by dissociation to CH_3O and NO. In the NM−DEA system, the data verify a chemical mechanism previously proposed by Gupta involving the NM aci-anion. Specifically, the observation of the protonated amine and its decomposition products demonstrates that the acid−base equilibrium step (reaction 1) is involved in the reaction mechanism, as is implied in many previous findings. We also directly detect trace amounts of the NM aci-anion, and its small signal level suggests that is it reactive and short-lived at the energies of our experiment. The data show that the NM−DEA reaction produces NO_2^- ions and that their production is correlated with an increase in the yield of methyl radicals. This result strongly suggests that $CH_3NO_2^-$ is the precursor of these products and provides direct evidence for reaction 4. Furthermore, the appearance of H/D atom exchanged products (facilitated by reactions 2 and 3) is consistent with the mechanism proposed by Gupta,[19] and the predicted magnitudes of these features based on that mechanism are also in very good quantitative agreement with our data. Because the protonated amine and its decomposition products account for all of the positively charged reaction products, other ionic mechanisms such as simple charge-transfer reactions or heterolytic bond cleavages must not contribute to the mechanism. Future work in this area will extend our study of nitroalkyl decomposition beyond the initial stages of reaction by increasing the size of the aerosol particles used as fuel. We will also expand the scope of this new technique to include more complex systems, such as RDX and ADN.

References and Notes

(1) Zhang, Y. X.; Bauer, S. H. *J. Phys. Chem. B* **1997**, *101*, 8717.
(2) Glaenzer, K.; Troe, J. *Helv. Chim. Acta* **1972**, *55*, 2884.
(3) Tsang, W.; Robaugh, D.; Mallard, W. G. *J. Phys. Chem.* **1986**, *90*, 5968.
(4) Wodtke, A. M.; Hintsa, E. J.; Lee, Y. T. *J. Phys. Chem.* **1986**, *90*, 3549.
(5) Zhao, X.; Hintsa, E. J.; Lee, Y. T. *J. Chem. Phys.* **1988**, *88*, 801.
(6) Tonnies, K.; Schmid, R. P.; Weickhardt, C.; Reif, J.; Grotemeyer, J. *Int. J. Mass Spectrom.* **2001**, *206*, 245.
(7) Blais, N. C. *J. Chem. Phys.* **1983**, *79*, 1723.
(8) Butler, L. J.; Krajnovich, D.; Lee, Y. T.; Ondrey, G.; Bersohn, R. *J. Chem. Phys.* **1983**, *79*, 1708.
(9) Ross, P. L.; van Bramer, S. E.; Johnston, M. V. *Appl. Spectrosc.* **1996**, *50*, 608.
(10) Wodtke, A. M.; Hintsa, E. J.; Lee, Y. T. *J. Chem. Phys.* **1986**, *84*, 1044.
(11) Eyster, E. H.; Smith, L. C.; Walton, S. R. US Navel Ordance Lab. Report No. NOLM 10336, 1949.
(12) Engelke, R.; Earl, W. L.; Rohlfing, C. M. *Int. J. Chem. Kinet.* **1986**, *18*, 1205.
(13) Engelke, R.; Schiferl, D.; Storm, C. B.; Earl, W. L. *J. Phys. Chem.* **1988**, *92*, 6815.
(14) Constantinou, C. P.; Mukundan, T.; Chaudhri, M. M. *Philos. Trans. R. Soc. London, Ser. A* **1992**, *339*, 403.
(15) Politzer, P.; Seminario, J. M.; Zacarias, A. G. *Mol. Phys.* **1996**, *89*, 1511.
(16) Cook, M. D.; Haskins, P. J. *Proc. 10th Symp. (Int.) Detonation* **1993**, 870.
(17) Blais, N. C.; Engelke, R.; Sheffield, S. A. *J. Phys. Chem. A* **1997**, *101*, 8285.
(18) Winey, J. M.; Gupta, Y. M. *J. Phys. Chem. A* **1997**, *101*, 9333.
(19) Gruzdkov, Y. A.; Gupta, Y. M. *J. Phys. Chem. A* **1998**, *102*, 2322.
(20) Cabalo, J.; Zelenyuk, A.; Baer, T.; Miller, R. E. *Aerosol Sci. Technol.* **2000**, *33*, 3.
(21) Zelenyuk, A.; Cabalo, J.; Baer, T.; Miller, R. E. *Anal. Chem.* **1999**, *71*, 1802.
(22) Noble, C. A.; Prather, K. A. *Environ. Sci. Technol.* **1996**, *30*, 0, 2667.
(23) Carson, P. G.; Neubauer, K. R.; Johnston, M. V.; Wexler, A. S. *J. Aerosol Sci.* **1995**, *26*, 535.
(24) Murphy, D. M.; Thomson, D. S. *Aerosol Sci. Technol.* **1995**, *22*, 237.

(25) Liu, P.; Ziemann, P. J.; Kittelson, D. B.; McMurry, P. H. *Aerosol Sci. Technol.* **1995**, *22*, 293.
(26) Liu, P.; Ziemann, P. J.; Kittelson, D. B.; McMurry, P. H. *Aerosol Sci. Technol.* **1995**, *22*, 314.
(27) Jayne, J. T.; Leard, D. C.; Zhang, X.; Davidovits, P.; Smith, K. A.; Kolb, C. E.; Worsnop, D. R. *Aerosol Sci. Technol.* **2000**, *33*, 49.
(28) Woods III, E.; Smith, G. D.; Dessiaterik, Y.; Baer, T.; Miller, R. E. *Anal. Chem.*, submitted.
(29) Woods III, E.; Smith G. D.; Miller, R. E.; Baer, T. Manuscript in preparation.
(30) Katsumata, S.; Shiromaru, H.; Mitani, K.; Iwata, S.; Kimura, K. *Chem. Phys.* **1982**, *69*, 423.
(31) Brill, T. B.; James, K. J. *Chem. Rev.* **1993**, *93*, 2667.
(32) Zhang, Y. X.; Bauer, S. H. *Int. J. Chem. Kinet.* **1999**, *31*, 655.
(33) Reiner, E. J.; Harrison, A.; Bowen, R. D. *Can. J. Chem.* **1989**, *67*, 2081.
(34) Engelke, R.; Earl, W. L.; Rohlfing, C. M. *J. Chem. Phys.* **1986**, *84*, 142.
(35) Lide, D. R. *CRC Handbook of Chemistry and Physics*, 81st ed.; CRC Press: Cleveland, 2000.
(36) Mallard, W. G.; Lindstrom, P. J.; Eds. In *NIST Chemistry WebBook*; NIST Standard Reference Database Number 69, February 2000 ed.; National Institute of Standards and Technology: Gaithersburg, MD, 2001.
(37) Compton, R. N.; Carman, Jr.; Desfancois, C.; Abdoul-Carmine, H.; Schermann, J. P.; Hendricks, J. H. *J. Chem. Phys.* **1996**, *105*, 3472.
(38) Hunter, E. P. L.; Lias, S. G. *J. Phys. Chem. Ref. Data* **1998**, *27*, 413.
(39) Metz, R. B.; Cyr, D. R.; Neumark, D. M. *J. Phys. Chem.* **1991**, *95*, 2900.
(40) Polasek, M.; Turecek, F. *J. Phys. Chem. A* **2001**, *105*, 1371.
(41) Ervin, K. M.; Ho, J.; Lineberger, W. C. *J. Phys. Chem.* **1988**, *92*, 5405.